



Time-variant reliability-based design optimization using sequential kriging modeling

Mingyang Li¹ · Guangxing Bai² · Zequn Wang¹

Received: 7 August 2017 / Revised: 12 February 2018 / Accepted: 13 February 2018 / Published online: 21 March 2018
© Springer-Verlag GmbH Germany, part of Springer Nature 2018

Abstract

This paper presents a sequential Kriging modeling approach (SKM) for time-variant reliability-based design optimization (tRBDO) involving stochastic processes. To handle the temporal uncertainty, time-variant limit state functions are transformed into time-independent domain by converting the stochastic processes and time parameter to random variables. Kriging surrogate models are then built and enhanced by a design-driven adaptive sampling scheme to accurately identify potential instantaneous failure events. By generating random realizations of stochastic processes, the time-variant probability of failure is evaluated by the surrogate models in Monte Carlo simulation (MCS). In tRBDO, the first-order score function is employed to estimate the sensitivity of time-variant reliability with respect to design variables. Three case studies are introduced to demonstrate the efficiency and accuracy of the proposed approach.

Keywords Time-variant reliability analysis · Design optimization · Stochastic processes · Simulation-based · Kriging surrogate model

Abbreviations

X	Random variables	$[0, T]$	Time interval
d	Design variables	cost(.)	Cost function
Y(t)	Stochastic processes	R	Reliability
$Y_G(t)$	Gaussian stochastic process	R_t	Reliability target
$Y_{NG}(t)$	Non-Gaussian stochastic process	CCL_t	User-defined cumulative confidence level target
$G(\cdot)$	Original limit state function	$\Phi(\cdot)$	Standard Gaussian cumulative distribution function
$g(\cdot)$	Transformed time-independent limit state function	$f_x(\cdot)$	Probability density function
$g_K(\cdot)$	Surrogate Kriging model	P_f	Probability of system failure
t	Time parameter	W	Input random variables [X , Y' , t'] of Kriging model
		D	Training data set
		Cov (,..)	Covariance matrix
		R	Correlation matrix

Responsible Editor: Nestor V. Queipo

✉ Zequn Wang
zequnw@mtu.edu

Mingyang Li
mli7@mtu.edu

Guangxing Bai
baigx20@gmail.com

¹ Department of Mechanical Engineering-Engineering Mechanics, Michigan Technological University, Houghton, MI 49931, USA

² Department of Industrial Engineering, Wichita State University, Wichita, KS 67260, USA

1 Introduction

Reliability-based design optimization (RBDO) has been widely applied in practical engineering applications to ensure system performance under various sources of uncertainty (Simpson and Martins 2011; Wu et al. 2001; Kim et al. 2006; Yu and Du 2006). Different optimization strategies have been proposed to efficiently carry out RBDO, including double-loop methods (Youn et al. 2005; Yang and Yi 2009; Lin et al. 2011), decoupled methods (Zou and Mahadevan 2006; Agarwal and

Renaud 2006), and single-loop methods (Shan and Wang 2008; Li et al. 2013; Mansour and Olsson 2016). In the double loop methods, the inner loop performs reliability analysis while the outer loop searches for optimum designs iteratively. To reduce the computational costs, decoupled approaches transform the RBDO problem to a sequence of deterministic optimization and reliability analysis while single-loop methods reformulate the RBDO problem by incorporating reliability constraints as the optimality conditions. In RBDO, reliability analysis plays a critical role, as it requires a considerable amount of computational efforts in evaluating an integration of probability density function over failure region. Vast efforts have been investigated to improve the effectiveness of reliability analysis from many aspects, such as the most probable point (MPP)-based approaches (Baran et al. 2013; Du and Hu 2012), dimension reduction (DR) methods (Won et al. 2009; Rahman and Xu 2004), polynomial chaos expansion (PCE) (Hu and Youn 2011; Ghanem and Spanos 2003), and surrogate-based methods (Gaspar et al. 2014; Wang and Wang 2013). As a MPP-based approach, FORM intends to locate the most probable point (MPP) which is defined as the closest point on the limit state from the origin in standard normal space (U-space), and approximate the probability of failure by linearizing the limit state function at MPP. Dimension reduction methods reduce the computational cost of reliability assessment by decomposing the multi-dimensional integration into multiple lower dimensional integrations. The PCE methods can predict the probability of failure more accurately with the construction of stochastic response surfaces while demanding extensive computational resources for high dimensional problems due to the curse of dimensionality.

Recently, time-variant RBDO (Wang et al. 2013; Singh et al. 2010) has gain an increasing attention for engineering system design. Time-variant RBDO, referred to as “tRBDO”, seeks optimum system designs with a high reliability level over time under time-variant uncertainties such as stochastic operation condition and system aging. Thus, the time-variant reliability analysis in tRBDO often involves stochastic processes and time parameters and thus is technically difficult and computationally expensive. In the literature, many methods have been developed for the time-variant reliability analysis. In the extreme value based approaches (Li et al. 2007; Zhang and Du 2011), the worst scenario of system performance over a time interval is extracted to identify system failures. A time-variant reliability model can be transformed to a time-independent counterpart by only focusing on extreme system performances, and static reliability analysis tools are employed to estimate the time-variant probability of failure. Chen and Li (2007) proposed an approach to evaluate the structural reliability based on the distribution of extreme value, where the virtual stochastic process is created to capture the probability density function of the extreme value. Hu and Du (2012) proposed a sampling method to evaluate the

extreme values of stochastic processes, and approximate the time-variant reliability using the first-order reliability method. As analytical-based approaches, the out-crossing rate-based approaches (Li and Der Kiureghian 1995; Sudret 2008) evaluate the time-variant probability of failure by the integration of an out-crossing rate. Kuschel and Rackwitz (2000a, b) approximated the out-crossing rate by asymptotic second-order reliability methods while Andrieu-Renaud et al. (2004) proposed a PHI2 approach to obtain time-invariant reliability indices using FORM and compute the outcrossing rate based on the correlation of reliability indices at two successive time instants. To solve the first passage problem in time-variant reliability analysis involving stationary random processes, Singh et al. (2011) developed an importance sampling approach to calculate the cumulative probability of failure. Recently, some researchers have utilized metamodeling techniques (Wang and Chen 2017; Majcher et al. 2015; Li and Wang 2017) to alleviate the computational burden of time-variant reliability analysis. With the consideration of parametric uncertainty, Hu et al. (2016) construct surrogate models for evaluating the time-instantaneous reliability index, and then identify the time-instantaneous most probable points using the fast integration method. Wang and Wang (2015) proposed a double-loop adaptive sampling approach for efficient time-variant reliability analysis. In detail, Gaussian process regression is adopted to build surrogate models for predicting extreme system responses over time while the double loop sampling scheme searches for input variables and time concurrently for updating the surrogate model until a pre-defined confidence target is satisfied. Hu and Du (2015) developed a simulation method to evaluate the time-variant reliability based on the first order approximation and series expansions, where the stochastic process of the system performance is mapped into a Gaussian process for efficiently approximating time-variant reliability.

Though vast efforts have been investigated for time-variant reliability assessment, a rigorous formulation is still lacking for generic time-variant reliability-based design optimization (tRBDO) and it remains a grand challenge to handle such complexity associated with both stationary and non-stationary stochastic processes in tRBDO. In this paper, a sequential Kriging modeling approach (SKM) is proposed to effectively search for optimal designs with the desired system time-variant reliability level over a time period under uncertainty. The major contribution of the proposed work lies in developing a simulation-based framework for efficiently handling the complexity and high dimensionality of generic stochastic processes in time-variant reliability-based design optimization. The SKM approach involves a transformation scheme for the dimension reduction of performance functions with stochastic processes, and thus enables the development of time-independent Kriging models in the transformed space to evaluate time-variant system reliability. A design-driven sequential sampling method is then developed for managing

the surrogate model uncertainty due to lack of data in tRBDO. The rest of the paper is organized as follows. Section 2 proposes the sequential Kriging modeling method for the time-variant reliability-based design optimization involving stochastic processes. In Section 3, three case studies are used to demonstrate the effectiveness of SKM approach.

2 Sequential kriging modeling approach

This section presents a sequential Kriging modeling approach (SKM) for probabilistic design under both uncertain parameters and stochastic processes. The framework of tRBDO with stochastic processes using the SKM approach is first introduced in Subsection 2.1, while the details of the proposed approach are discussed in the following subsections.

2.1 Time-variant RBDO framework

In engineering design, various sources of uncertainties must be considered to ensure a high-level of system reliability; however, time-related uncertainties such as stochastic operating conditions and component deteriorations have not been taken into account in RBDO. Therefore, time-variant RBDO (tRBDO) is introduced to obtain optimum solutions with the minimum cost while satisfying system reliability requirements over a time period. Generally, a time-variant RBDO with stochastic processes $\mathbf{Y}(t)$ and time parameter t can be formulated as

$$\begin{aligned}
 & \text{Minimize : } Cost(\mathbf{X}, \mathbf{d}) \\
 & \text{subject to : } P_f(0, T) = \Pr(\exists t \in [0, T], G_i(\mathbf{X}, \mathbf{d}, \mathbf{Y}(t), t) \leq 0) \\
 & \leq 1 - R_t, i = 1, \dots, nc \tag{1} \\
 & \mathbf{Y}(t) = [Y_1(t), Y_2(t), \dots, Y_{ns}(t)] \\
 & \mathbf{d}^L \leq \mathbf{d} \leq \mathbf{d}^U, \mathbf{d} \in R^{nd} \text{ and } \mathbf{X} \in R^{nr}
 \end{aligned}$$

where $Cost(\mathbf{X}, \mathbf{d})$ is the object function and $[0, T]$ is the projected lifetime; $\mathbf{Y}(t)$ represents a vector of stochastic processes; $G_i(\mathbf{X}, \mathbf{d}, \mathbf{Y}(t), t) \leq 0$ is defined as the i^{th} failure mode and $P_f(0, T)$ is the time-variant probability of failure at time interval $[0, T]$; \mathbf{d} is a vector of design variables and \mathbf{X} is a vector of random variables; \mathbf{d}^L and \mathbf{d}^U are the lower and upper boundaries of the design variables; nc , nd , ns , and nr are the numbers of constraints, design variables, stochastic processes, and random variables, respectively.

The proposed sequential Kriging modeling framework aims to handle tRBDO involving stochastic processes, which mainly consists of four critical components: (1) stochastic processes modeling, (2) stochastic equivalent transformation to handle the high dimensionality associated with temporal uncertainty, (3) design-driven adaptive sampling, and (4) stochastic sensitivity analysis. To solve a tRBDO problem, a deterministic

design optimization problem is first solved to obtain the initial design point. Starting with the deterministic optimum design as shown in Fig. 1, the SKM first generates realizations of stochastic processes according to their probabilistic characterizations, and then translates time-variant reliability models to time-independent counterparts through the stochastic equivalent transformation. It is worth noting that the resulting time-independent reliability model can predict time-variant system performance and thus is capable of capturing time-variant failures in time domain. Kriging surrogate model is then constructed for the time-independent reliability model and updated by identifying important samples across time-design domain. To evaluate the time-variant reliability, the resulting Kriging models will be mapped back to time-variant space for predicting time-variant system performance, which eventually yields the extreme distributions of system performance and time-variant probability of failure. The sensitivity of time-variant reliability with respect to design variables is approximated based on the first-order score function, and then utilized in the optimizer to search for optimum designs iteratively.

2.2 Random processes realization

In SKM, the first step is to generate random realizations of stochastic processes, including Gaussian/non-Gaussian and/or stationary/non-stationary random processes. For a stochastic process such as Gaussian process $Y_G(t)$, it can be prescribed by

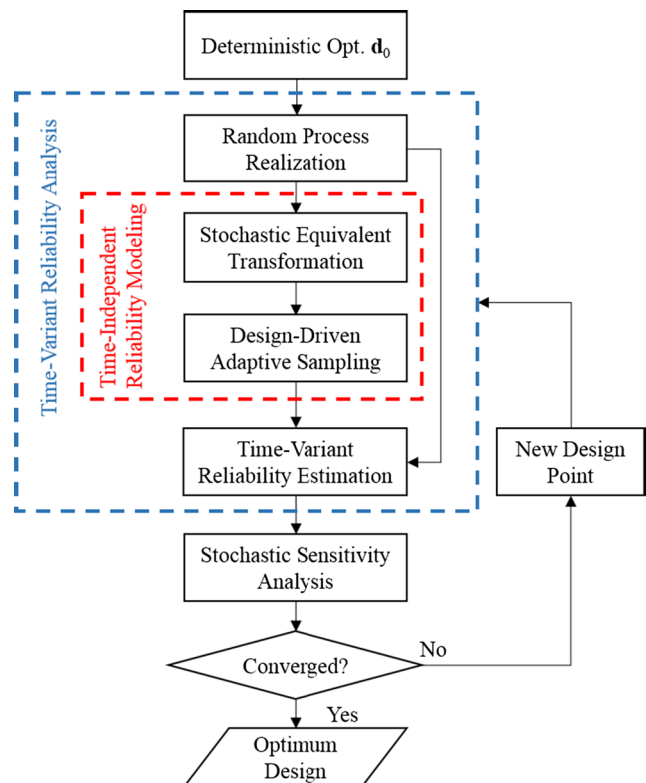


Fig. 1 Flowchart of SKM framework for tRBDO

three functions with respect to time t , mean function $\mu_Y(t)$, standard deviation function $\sigma_Y(t)$, and auto correlation function $\rho_Y(t)$. In the literature, various methods (Sakamoto and Ghanem 2002a, b; Saul and Jordan 1999) can be used to simulate a Gaussian process, such as the Expansion Optimal Linear Estimation method (EOLE) (Zhang et al. 2017), and the Orthogonal Series Expansion method (Zhang and Ellingwood 1994) (OSE). Assuming the time interval is discretized by s time nodes, the covariance between two time nodes is calculated by

$$Cov(t_i, t_j) = \sigma_Y(t_i)\sigma_Y(t_j)\rho_Y(t_i, t_j) \tag{2}$$

then the corresponding covariance matrix is derived as

$$\Sigma = \begin{pmatrix} Cov(t_1, t_1) & Cov(t_1, t_2) & \cdots & Cov(t_1, t_s) \\ Cov(t_2, t_1) & Cov(t_2, t_2) & \cdots & Cov(t_2, t_s) \\ \vdots & \vdots & \ddots & \vdots \\ Cov(t_s, t_1) & Cov(t_s, t_2) & \cdots & Cov(t_s, t_s) \end{pmatrix} \tag{3}$$

The covariance matrix can be decomposed as $\Sigma = \mathbf{Q}\mathbf{I}\mathbf{Q}^T$ by using Eigen decomposition where $\mathbf{Q} = [\mathbf{Q}_1, \mathbf{Q}_2, \dots, \mathbf{Q}_s]$ is the matrix of eigenvectors and \mathbf{I} is a diagonal matrix with the corresponding eigenvalues. Then the Gaussian process $Y_G(t)$ can be expressed as

$$Y_G(t) \approx \mu_Y(t) + \sum_{i=1}^p \sqrt{I_i} Q_i(t) Z_i \tag{4}$$

where p is the number of dominated Eigen functions and $\mathbf{Z} = [Z_1, Z_2, \dots, Z_p]$ are a set of uncorrelated standard normal random variables.

For non-Gaussian processes, Polynomial Chaos Expansion (PCE) and Karhunen-Loeve (KL) expansion are adopted in this paper to generate random realizations. According to the methodology in Sakamoto and Ghanem (2002a), a non-Gaussian process $Y_{NG}(t)$ can be approximated by Hermite orthogonal polynomials, which is expressed as

$$Y_{NG}(t) = \sum_{s=0}^p b_s(t) \Psi_s(\xi(t)) \tag{5}$$

where the Hermite polynomials $\Psi_s(\xi(t))$ are expressed as

$$\Psi_s(\xi(t)) = (-1)^s \frac{\phi^s(\xi(t))}{\phi(\xi(t))} \tag{6}$$

where $\phi^s(\xi(t))$ is the s^{th} derivative of probability density function of the standard normal process $\xi(t)$. Then, the approximation of $Y_{NG}(t)$ can be written as

$$Y_{NG}(t) = \sum_{s=0}^p b_s(t) \Psi_s(\xi(t)) = b_0(t) + b_1(t)\xi(t) + b_2(t)(\xi^2(t)-1) + b_3(t)(\xi^3(t)-3\xi(t)) + \dots \tag{7}$$

where $b_s(t), s = 0, 1, 2, 3$ are expansion coefficients corresponding to the first four moments of the non-Gaussian process $Y_{NG}(t)$. For a given non-Gaussian process, the mean $\mu_{NG}(t)$, standard deviation $\sigma_{NG}(t)$, skewness $Sk_{NG}(t)$, and kurtosis $K\mu_{NG}(t)$ are used to calculate the expansion coefficients $b_s(t)$. Assuming that a non-Gaussian process $Y_{NG}(t)$ is expanded in a four-terms series ($s = 3$), the first coefficient $b_0(t)$ is equal to $\mu_{NG}(t)$ as the mean values of the Hermite polynomials are zero. According to the orthonormality properties of the Hermite polynomials, the i^{th} central moments ($i = 2, 3, 4$) can be expressed as,

$$gg_i(b_1(t), b_2(t), b_3(t)) = E[(Y_{NG}(t)-b_0)^i], i = 2, 3, 4 \tag{8}$$

The values of $b_1(t), b_2(t)$, and $b_3(t)$ is obtained by minimizing the difference between the gg_i values and the given moments, expressed as

$$\min_{b_1, b_2, b_3} \sum_{i=2}^4 (gg_i(b_1(t), b_2(t), b_3(t)) - M_i) \tag{9}$$

where M_i are the i^{th} central moments of the given non-Gaussian process $Y_{NG}(t)$. It is worth noting that the expansion coefficients $b_s(t)$ are time independent if the non-Gaussian process is stationary. Using the orthogonality properties of the Hermite polynomials, the relationship between covariance matrix $C_{NG}(t_i, t_j)$ of $Y_{NG}(t)$ and covariance matrix $C_\xi(t_i, t_j)$ of $\xi(t)$ can be written as

$$C_{NG}(t_i, t_j) = \sum_{s=1}^3 b_s^2(t) \cdot (s!) \cdot (C_\xi(t_i, t_j))^s \tag{10}$$

Given that $C_{NG}(t_i, t_j)$ can be analytically determined based on the autocorrelation of random process $Y_{NG}(t)$, the covariance matrix of the standard normal process $C_\xi(t_i, t_j)$ can be computed according to (10). A KL expansion is then able to represent $\xi(t)$ as

$$\xi(t) = \sum_{i=1}^p \sqrt{\lambda_i} f_i(t) \xi_i \tag{11}$$

where p is the number of dominant eigenvalues, λ_i and $f_i(t)$ are the eigenvalues and eigenvectors of covariance matrix $C_\xi(t_i, t_j)$, and ξ_i are independent standard normal random variables.

A stationary non-Gaussian process $Y_{NG}(t)$ following a Weibull marginal PDF with the shape parameter 1.5 and scale parameter 3 is simulated to generate fifteen random realizations as shown in Fig. 2. The autocorrelation function is expressed as

$$\rho_{NG}(\Delta t) = e^{-\left(\frac{\Delta t}{0.5}\right)^2} \tag{12}$$

where the given time interval $[0, 1]$ is discretized into 100 time nodes. With the first four moments $\mu_{NG} = 2.7082, \sigma_{NG} =$

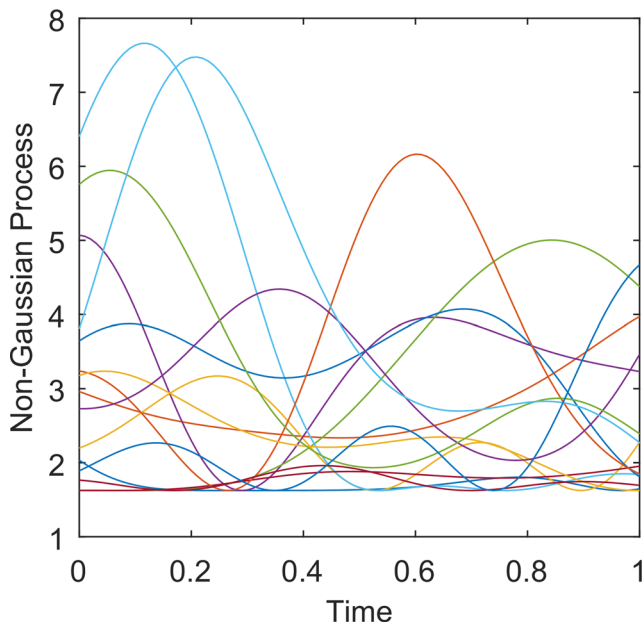


Fig. 2 Fifteen random realizations of the non-Gaussian process

1.8388, $Sk_{NG} = 1.0720$, and $K\mu_{NG} = 1.3904$, a series of Hermite polynomials is used to represent the stochastic process with the four expansion coefficients estimated by (9), expressed as

$$Y_{NG}(t) = 2.7082 + 0.9662\xi(t) + 0.5652(\xi^2(t)-1) - 0.0575(\xi^3(t)-3\xi(t)) \quad (13)$$

With the obtained four expansion coefficients, the covariance matrix of $\xi(t)$ is calculated by (10). Through employing the Eigen analysis, the standard normal process $\xi(t)$ is then generated from the KL expansion with five dominate Eigen values as shown in Fig. 3.

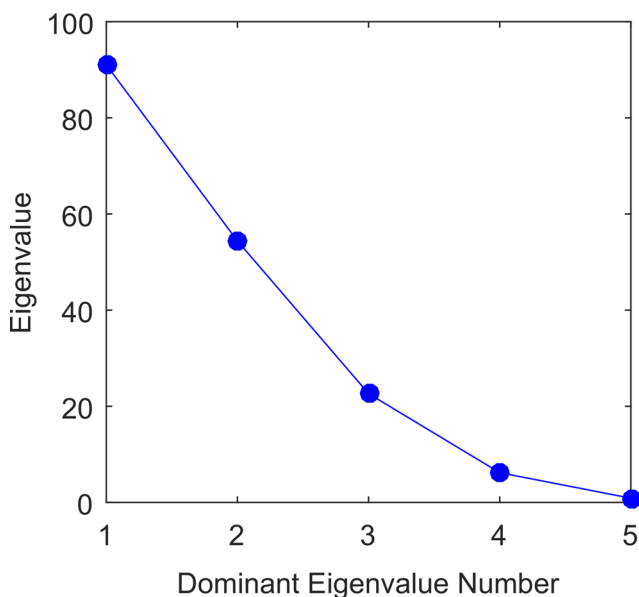


Fig. 3 Five dominate eigenvalues in the KL expansion

2.3 Stochastic equivalent transformation

In the time-variant reliability analysis, the limit state is a function of random inputs \mathbf{X} , stochastic processes $\mathbf{Y}(t)$, and time parameter t . In SKM, stochastic equivalent process transformation (Wang and Chen 2016) transforms the origin time-variant limit state function $G(\mathbf{X}, \mathbf{Y}(t), t)$ to a time-independent domain, and instantaneous failure events are described as

$$g(\mathbf{X}, \mathbf{Y}', t') < 0 \quad (14)$$

where continuous random variables \mathbf{Y}' and t' are translated from stochastic processes $\mathbf{Y}(t)$ and time t respectively, random variables \mathbf{X} remain the same in the transformed input space. As shown in Fig. 4, with the multiple realizations of the stochastic process $Y(t)$, the probability density function (PDF) of Y' is then obtained by averaging the PDFs of $Y(t)$ over the time of interest $[0, T]$. At each time node, the stochastic process is converted to a random variable, and thus the transformed random parameter Y' is a mixture model constructed with random distributions at a set of time nodes. By discretizing the time interval into s time nodes, s probability density function can be obtained for the distribution of $Y(t_i), i = 1, 2, \dots, s$. The probability density function of the Y' is then expressed as

$$f_{pdf}(Y') \approx \frac{1}{s} \sum_{i=1}^s f_{pdf}(Y(t_i)) \quad (15)$$

For stationary Gaussian processes, the probabilistic characteristics of Y' can be obtained analytically as the mean and standard deviation functions remain the same over time. In terms of general random processes, the realizations of stochastic processes $Y(t)$ in Subsection 2.2 is readily merged to form a set of random sample points that follow the distribution of

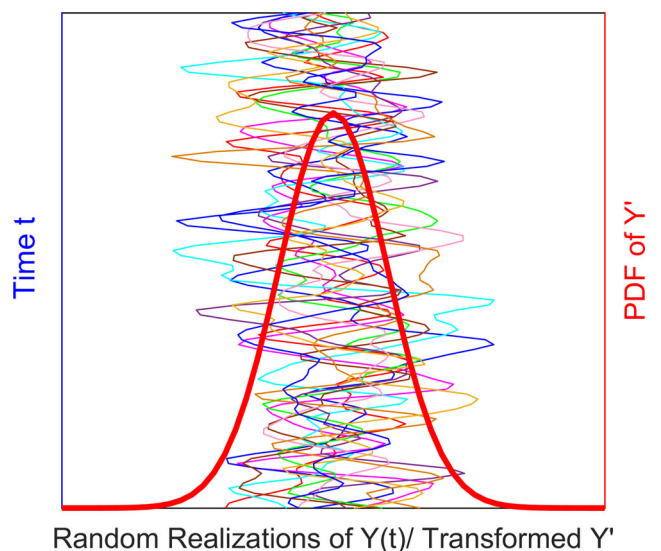


Fig. 4 Transformation of stochastic process $\mathbf{Y}(t)$

random parameter Y' . In the transformed input space, the random variable t' is treated as a uniform distributed variable over the time interval $[0, T]$ as a failure event at any time instant will lead to a system failure.

With the transformed random parameters \mathbf{X} , \mathbf{Y}' , and t' , the probability of failure in the transformed space is defined as

$$P_{f-ave} = \Pr \left[g(\mathbf{X}, \mathbf{Y}', t') < 0 \right] \tag{16}$$

where the P_{f-ave} is the average of the instantaneous probability of failure over the time interval $[0, T]$. It is worth noting that the time-independent model in (14) is able to capture time-variant failure events by nature.

2.4 Design-driven adaptive sampling

With the stochastic equivalent transformation, surrogate modeling techniques are employed to predict the time-independent limit state function $g(\mathbf{X}, \mathbf{Y}', t')$. Though a variety of surrogate modeling techniques are available, a confidence-based adaptive sampling scheme (Wang and Chen 2017) is utilized in the proposed approach to construct metamodels for the time-independent limit state function mainly due to its ability of efficiently handling surrogate model uncertainty. Let $\mathbf{W} = [\mathbf{X}, \mathbf{Y}', t']$ denotes the input variables of transformed limit state function $g(\mathbf{X}, \mathbf{Y}', t')$, and \mathbf{w} is a random realization of input \mathbf{W} , the probability of failure is then expressed as

$$P_{f-ave} = \Pr(g(\mathbf{w}) < 0) = \int \dots \int_{g(\mathbf{w}) < 0} f_x(\mathbf{w}) d\mathbf{w} \tag{17}$$

where $f_x(\mathbf{w})$ is the joint probability density function. By defining the failure region $\Omega_f = \{\mathbf{w} \mid g(\mathbf{w}) < 0\}$, the probability of failure can be expressed as

$$P_{f-ave} = \Pr(\mathbf{w} \in \Omega_f) = \int_{\Omega} I_f(\mathbf{w}) f_x(\mathbf{w}) d\mathbf{w} = E[I_f(\mathbf{w})] \tag{18}$$

where Ω represents the transformed random input space. $E[\cdot]$ is the expectation operator and $I_f(\mathbf{w})$ is an indicator function to classify success and failure points, defined as

$$I_f(\mathbf{w}) = \begin{cases} 1, & \mathbf{w} \in \Omega_f \\ 0, & \text{otherwise} \end{cases} \tag{19}$$

Let n_r and n_s denote the number of random variables in \mathbf{X} and \mathbf{Y}' respectively, then $k = n_r + n_s + 1$ is the number of input variables in \mathbf{W} . With the training data set $\mathbf{D} = [\mathbf{W}, \mathbf{G}]$ consisting of n input points \mathbf{W} and the corresponding responses \mathbf{G} , the general form of Kriging model is described as

$$g_K(\mathbf{w}) = f(\mathbf{w}) + S(\mathbf{w}) \tag{20}$$

where $g_K(\mathbf{w})$ is the approximation of the performance function $g(\mathbf{w})$ at the point \mathbf{w} . The first term $f(\mathbf{w})$ is a polynomial term which can be substituted by a constant

value μ . $S(\mathbf{w})$ is a Gaussian stochastic process with zero mean and a covariance matrix given by

$$\mathbf{Cov}_{(i,j)} = \sigma^2 \mathbf{R} \tag{21}$$

where i and j represent input points \mathbf{w}_i and \mathbf{w}_j , respectively, and \mathbf{R} is a $n \times n$ correlation matrix. Various correlation functions are available in the literature, such as Gaussian, rational quadratic, Matern, and exponential correlation function. According to Stein (1988), the impact on the Kriging prediction from not using the suitable covariance structure is asymptotically negligible if the Kriging model can be updated by having more observations. In this study, the Kriging surrogate will be iteratively updated by the adaptive sampling scheme. Thus, the selection of the Kriging covariance structure will not have significant impact on the response prediction, and a stationary and isotropic Gaussian correlation function is adopted in this paper, expressed as

$$R(\mathbf{w}_i, \mathbf{w}_j) = \exp \left[- \sum_{q=1}^k a_q |\mathbf{w}_{i,q} - \mathbf{w}_{j,q}|^{b_q} \right] \tag{22}$$

With n initial samples $[\mathbf{W}, \mathbf{G}]$, the log likelihood function is given by

$$\begin{aligned} \text{LogLikelihood} = & \\ & - \frac{1}{2} \left[n \ln(2\pi) + n \ln \sigma^2 + \ln |\mathbf{R}| + \frac{1}{2\sigma^2} (\mathbf{G} - \mathbf{A}\mu)^T \mathbf{R}^{-1} (\mathbf{G} - \mathbf{A}\mu) \right] \end{aligned} \tag{23}$$

where \mathbf{A} is an $n \times 1$ unit vector. All the hyper parameters can be obtained by maximizing the likelihood function, and then the correlation matrix \mathbf{R} can be computed according to (22). Let \mathbf{r} denotes the correlation vector between a new point \mathbf{w}' and training samples, the response and mean square error predicted by the Kriging model are obtained as

$$g_k(\mathbf{w}') = \mu + \mathbf{r}^T \mathbf{R}^{-1} (\mathbf{G} - \mathbf{A}\mu) \tag{24}$$

$$e(\mathbf{w}') = \sigma^2 \left[1 - \mathbf{r}^T \mathbf{R}^{-1} \mathbf{r} + \frac{(1 - \mathbf{A}^T \mathbf{R}^{-1} \mathbf{r})^2}{\mathbf{A}^T \mathbf{R}^{-1} \mathbf{A}} \right] \tag{25}$$

To handle the surrogate model uncertainty $e(\cdot)$ due to the lack of data, adaptive sampling scheme should be employed for identifying most useful point and updating Kriging for probability analysis in Monte Carlo simulation (MCS).

In MCS, N Monte Carlo samples are generated based on the randomness of the input variables, denoted as

$$\mathbf{w}_{m,i} = [\mathbf{x}_i, \mathbf{y}_i^{mcs}, t_i], i = 1, 2, \dots, N \tag{26}$$

where \mathbf{y}_i^{mcs} is the i^{th} Monte Carlo samples of \mathbf{Y}' . For the point $\mathbf{w}_{m,i}$, the limit state function $g(\mathbf{w}_{m,i})$ can be approximated by

Kriging as a normally distributed random variable, given by $g(\mathbf{w}_{m,i}) \sim N(g_k(\mathbf{w}_{m,i}), e(\mathbf{w}_{m,i}))$. The indicator function is thus derived as

$$I_f(\mathbf{w}_{m,i}) = \begin{cases} 1, & g_k(\mathbf{w}_{m,i}) < 0 \quad (\text{failure}) \\ 0, & g_k(\mathbf{w}_{m,i}) \geq 0 \quad (\text{success}) \end{cases} \quad (27)$$

The average probability of failure P_{f-ave} , over the time period $[0, T]$ is thus calculated in MCS. The confidence level (CL) at the point $\mathbf{w}_{m,i}$ is defined as the probability of correct classification, which is expressed as

$$CL(\mathbf{w}_{m,i}) = \Phi\left(\frac{|g_k(\mathbf{w}_{m,i})|}{\sqrt{e(\mathbf{w}_{m,i})}}\right) \quad (28)$$

where $\Phi(\cdot)$ is a standard normal cumulative distribution function. After evaluating the CL for all the points in MCS, the cumulative confidence level (CCL) is obtained as

$$CCL = \frac{1}{N} \sum_{i=1}^N CL(\mathbf{w}_{m,i}) \quad (29)$$

The CCL indicates the accuracy of Kriging model in predicting P_{f-ave} in MCS. To enhance the fidelity of Kriging model, the most useful point will be identified by maximizing the importance measure, which is defined as

$$H(\mathbf{w}_{m,i}) = (1-CL(\mathbf{w}_{m,i})) * f_x(\mathbf{w}_{m,i}) * \sqrt{e(\mathbf{w}_{m,i})} \quad (30)$$

where $f_x(\cdot)$ is the joint probability density function of input variables, and $e(\cdot)$ is the estimated mean square error of Kriging model prediction. The limit state value at the selected point will be evaluated and then incorporated in the training data set for updating the Kriging model. As shown in Fig. 5, the design-driven adaptive updating procedure will be triggered at each design iteration to search for the important sample points.

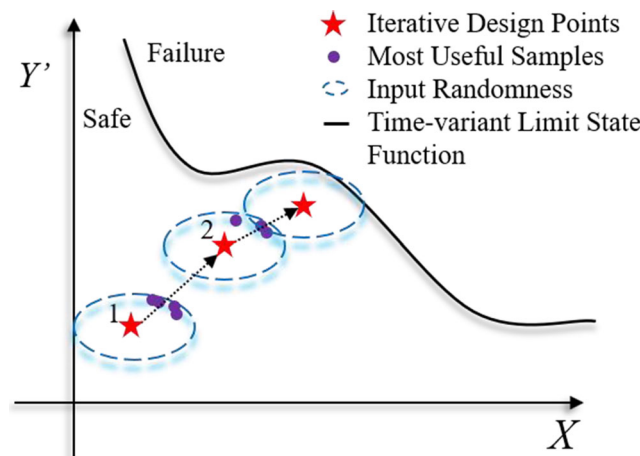


Fig. 5 Illustration of the design-driven adaptive sampling

2.5 Time-variant reliability analysis

With the Kriging surrogate model, the time-variant probability of failure within the time interval $[0, T]$ can be approximated by

$$P_f(0, T) \approx \Pr(\exists t \in [0, T], g_k(\mathbf{X}, \mathbf{Y}(t), t) < 0) \quad (31)$$

where $g_k(\cdot)$ is the time-variant limit state prediction using the Kriging model. Monte Carlo simulation (MCS) method is employed in this work to calculate the time-variant probability of failure in (31). In MCS, the first step is to generate N random realizations of \mathbf{X} and $\mathbf{Y}(t)$ as introduced in Section 2.2 by discretizing the time interval $[0, T]$ with s nodes. For the i^{th} realization of random parameter and the stochastic process $(\mathbf{x}_i, \mathbf{y}_i)$, the instantaneous limit state function $g(\mathbf{x}_i, \mathbf{y}_i, t_j)$ at the j^{th} time node is predicted directly by the Kriging model, and a time-variant failure event occurs if

$$\min_{1 \leq j \leq s} g_k(\mathbf{x}_i, \mathbf{y}_i, t_j) < 0 \quad (32)$$

Clearly, the distribution of the worst performance over time period $[0, T]$ can be obtained in (32), and the time-variant probability of failure is then approximated by

$$P_f(0, T) \approx \frac{N_f}{N} \quad (33)$$

where N_f is the number of time-variant failure samples within the time interval $[0, T]$.

2.6 Sensitivity analysis of time-variant reliability

In sensitivity analysis, a general form of the time-variant probability of failure is rewritten as

$$P_f(0, T) \equiv \int_{R^N} I_{f-t}(\mathbf{X}) f_x(\mathbf{X}) d\mathbf{X} = E[I_{f-t}(\mathbf{X})] \quad (34)$$

where \mathbf{X} is the vector of input random variables, $f_x(\mathbf{X})$ is the joint probability density function, and $I_{f-t}(\mathbf{X})$ is the indicator function expressed as

$$I_{f-t}(x_i) = \begin{cases} 1, & \min_{1 \leq j \leq s} g_k(x_i, y_j, t_j) < 0 \quad (\text{failure}) \\ 0, & \text{otherwise} (\text{success}) \end{cases} \quad (35)$$

The partial derivative of the probability of failure with respect to the i^{th} design variable d_i is thus derived (Hu et al. 2013) as

$$\begin{aligned} \frac{\partial P_f(0, T)}{\partial d_i} &= \frac{\partial}{\partial d_i} \int_{R^N} I_{f-t}(\mathbf{X}) f_x(\mathbf{X}) d\mathbf{X} \\ &= E \left[I_{f-t}(\mathbf{X}) \frac{\partial \ln f_x(\mathbf{X})}{\partial d_i} \right] \end{aligned} \quad (36)$$

For independent random variables, the joint probability density function of \mathbf{X} is expressed as multiplication its marginal PDFs as

$$f_x(\mathbf{X}) = \prod_{i=1}^{nr} f_{x_i}(x_i) \tag{37}$$

where nr is the dimension of input variables \mathbf{X} . With the time-variant reliability and its sensitivity information, the sequential quadratic programming (SQP) (Nocedal and Wright 2006) is adopted as an optimizer to search for optimum solutions iteratively in tRBDO.

3 Case studies

In this section, three examples are used to demonstrate the effectiveness of the proposed approach for solving the time-variant reliability-based design optimization problems.

3.1 Case study I: a mathematical design problem

A two dimensional mathematical time-variant reliability-based design optimization problem (Li et al. 2013) is formulated as

$$\begin{aligned} \text{Minimize : } & Cost(\mathbf{d}) = 10 - X_1 + X_2 \\ \text{subject to : } & P_f(0, 1) = \Pr(\exists t \in [0, 1], G_i(\mathbf{d}, Y_1(t), Y_2(t)) \leq 0) \\ & \leq 1 - R_t, i = 1 \sim 3 \\ & \mathbf{d} = [X_1, X_2], 0 \leq X_1 \& X_2 \leq 10 \end{aligned} \tag{38}$$

where

$$G_1 = \frac{X_1^2 X_2 - 1}{20}$$

$$G_2 = \frac{(X_1 + X_2 - 5)^2}{30} + \frac{(X_1 - X_2 - 12)^2}{120} - 1 - Y_1(t) + 0.01^* Y_2(t)$$

$$G_3 = \frac{80}{(X_1^2 + 8X_2 - 5)} - 1$$

where the two random design variables X_1 and X_2 follow normal distributions as $X_1 \sim N(\mu_1, 0.3464^2)$ and $X_2 \sim N(\mu_2, 0.3464^2)$. The target reliability is set to $R_t = 0.985$ for all three probabilistic constraints. To maintain a high-fidelity Kriging

model during the design optimization, a high-level target cumulative confidence level $CCL_t = 0.999$ is set as a criterion in updating Kriging models adaptively, as introduced in Subsection 2.4. The tRBDO problem involves two stochastic processes $\mathbf{Y}(t) = [Y_1(t), Y_2(t)]$, including a non-stationary Gaussian process $Y_1(t)$ and a stationary process $Y_2(t)$ with a Weibull marginal PDF. The Gaussian process $Y_1(t)$ is fully characterized by its mean function $\mu_Y(t)$, standard deviation function $\sigma_Y(t)$ and the autocorrelation function $\rho_Y(t)$, given as

$$\mu_Y(t) = 0.1^* t \tag{39}$$

$$\sigma_Y(t) = 0.05^* t \tag{40}$$

$$\rho_Y(t_1, t_2) = \exp\left(-\frac{(t_2 - t_1)^2}{0.001}\right) \tag{41}$$

The scale and shape parameters of the non-Gaussian process $Y_2(t)$ are set to 2 and 1.2, thus the first four moments can be directly obtained as mean $\mu_{NG} = 1.8813$, standard deviation $\sigma_{NG} = 1.5745$, skewness $Sk_{NG} = 1.5211$, and kurtosis $K\mu_{NG} = 3.2357$. The autocorrelation function of $Y_2(t)$ is given by

$$\rho_{NG}(t_1, t_2) = \exp\left(-\frac{(t_2 - t_1)^2}{0.01}\right) \tag{42}$$

Following the procedure outlined in subsection 2.2, the time interval $[0, 1]$ is discretized into 100 nodes evenly, and 10^6 random realizations for each stochastic process are generated for the time-variant reliability analysis. The first fifty realizations of $Y_1(t)$ and $Y_2(t)$ are shown in Fig. 6.

The first step of the SKM approach is to obtain an initial design point by solving the corresponding deterministic optimization problem, where the stochastic processes in G_2 are fixed to its mean. The deterministic design optimization starts with $\mathbf{d}_0 = [5, 5]$, and approaches the deterministic optimum design $\mathbf{d}_d = [8.5770, 1.4294]$ after seven iterations. As the second constraint G_2 contains stochastic processes, the time-variant limit state function of G_2 is converted to the time-

Fig. 6 50 realizations of the $Y_1(t)$ and $Y_2(t)$

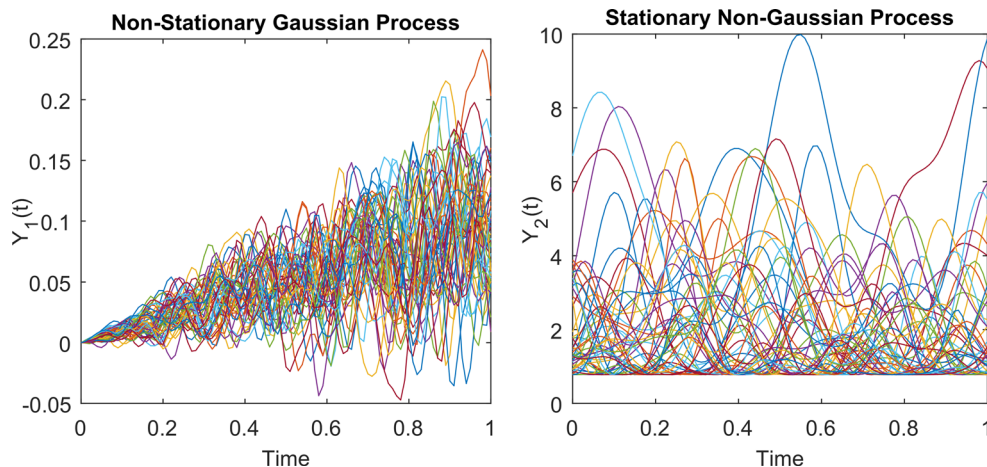


Table 1 tRBDO design history for case study I

Iterations	Design variables		Reliabilities			Cost
	X_1	X_2	R_1^{SKM}	R_2^{SKM}	R_3^{SKM}	
1	8.5770	1.4294	0.9995	0.2714	0.4990	2.8524
2	7.3334	3.0961	1	0.9771	0.8649	5.7627
3	7.0291	3.2763	1	0.9844	0.9497	6.2472
4	6.8607	3.3431	1	0.9851	0.9765	6.4824
5	6.7868	3.3676	1	0.9850	0.9839	6.5807
6	6.7732	3.3721	1	0.9850	0.9849	6.5989
7	6.7732	3.3720	1	0.9850	0.9849	6.5988
8	6.7733	3.3718	1	0.9850	0.9849	6.5985

independent one using stochastic equivalent transformation. The input domains of three Kriging models g_{K1} , g_{K2} , and g_{K3} are defined as $W_1 = W_3 = [X_1, X_2]$, $W_2 = [X_1, X_2, Y_1', Y_2']$, respectively, where the PDFs of Y_1' and Y_2' are obtained as introduced in Subsection 2.3. Then the Latin Hypercube sampling method (LHS) is utilized to generate 20 initial sample points, and they are combined with seven sample points that evaluated during deterministic design for constructing initial Kriging models. By setting the deterministic optimum design d_d as the initial design point in tRBDO, the optimum design $d_{opt} = [6.7733, 3.3718]$ is obtained after 8 iterations. The iterative history of reliabilities for three constraints, design points, and cost function values are summarized in Table 1. It is worth noting that the reliabilities are estimated by the updated Kriging models, denoted by R_1^{SKM} , R_2^{SKM} , and R_3^{SKM} , respectively.

During the tRBDO process, the design-driven adaptive sampling scheme is triggered to identify 57 samples and 9 samples for updating the Kriging model g_{K2} and g_{K3} ,

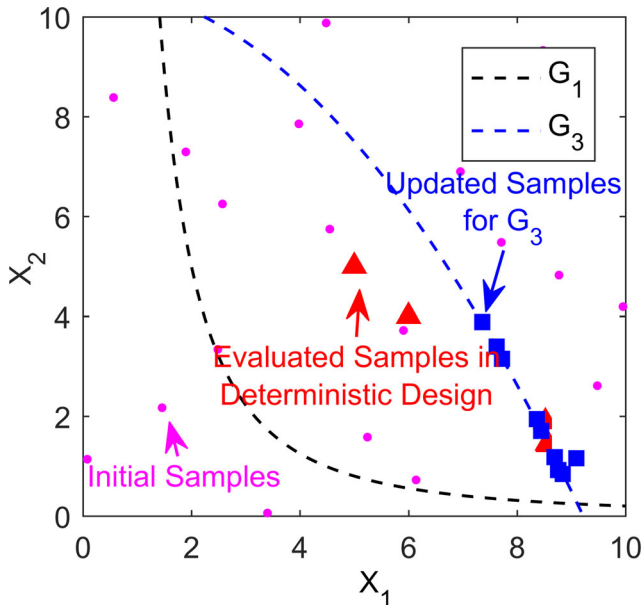


Fig. 7 Samples for constructing g_{K1} and g_{K3} Kriging models

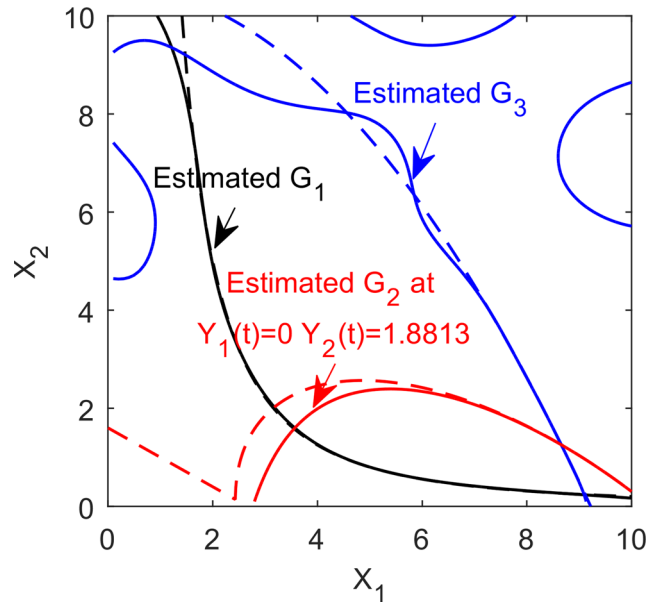


Fig. 8 Approximated limit state functions by Kriging model vs. true limit state functions

respectively. There is no need to update g_{K1} since the target CCL_t can always be satisfied in the design optimization process. Figure 7 shows the sample points for constructing the Kriging models, including 20 LHS samples, 7 samples evaluated during deterministic design optimization, and the additional nine samples identified through design-driven adaptive sampling for g_{K3} . The comparison between true limit state functions (dashed lines) and estimated results (solid lines) by updated Kriging models is shown in Fig. 8, where the time-variant limit state function G_2 is depicted at $Y_1(t) = 0$ and $Y_2(t) = 1.8813$. A high accuracy level of Kriging model g_{K2} can be obtained in the area near the optimum design

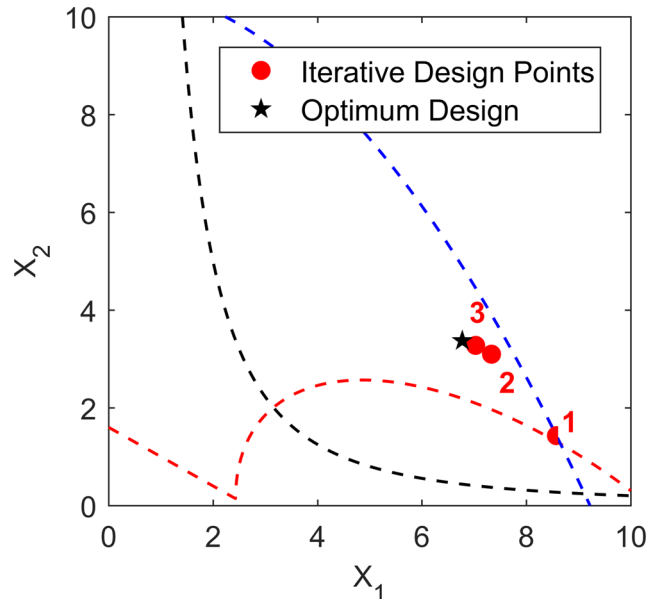


Fig. 9 Iterative design points in tRBDO

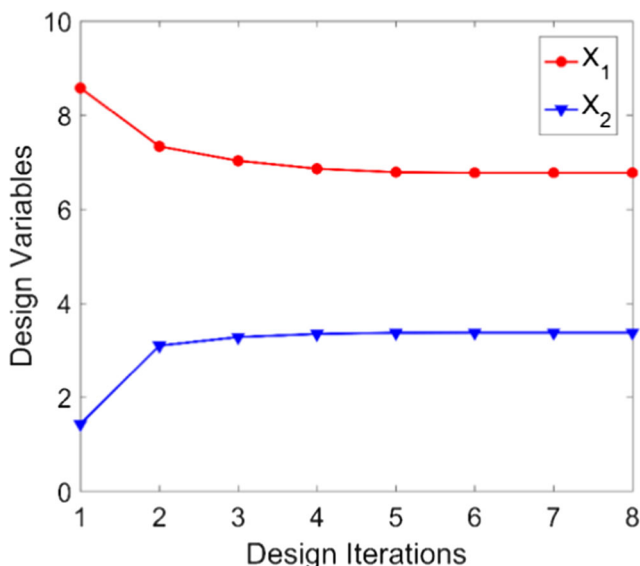


Fig. 10 Design history at each iteration

$\mathbf{d}_{opt} = [6.7733, 3.3718]$ because the most useful samples selected by the design-driven adaptive sampling scheme are located in the critical area of interest as needed.

The overall tRBDO process is shown in Fig. 9, where the first three designs are marked with numbers and point ‘1’ is the deterministic optimum design point. The convergence of design points with respect to design iterations is detailed in Fig. 10 while the time-variant reliabilities for three constraints also converge to the target reliability 0.9850 within 8 design iterations as shown in Fig. 11.

For the purpose of comparison, the simulation-based time-variant reliability analysis approach SPCE (Hu et al. 2013), together with the first-order score function method (SF) for sensitivity analysis, are employed to solve the same tRBDO

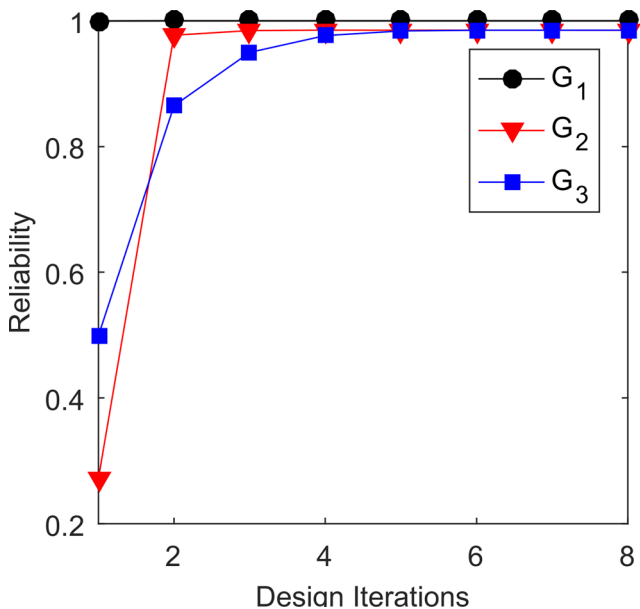


Fig. 11 Reliabilities of three constraints at each design iteration

Table 2 Comparison of optimum results for case study I

	Optimum	R_1	R_2	R_3	Cost	#F
SKM	[6.7733, 3.3718]	1	0.9839	0.9849	6.5984	147
SPCE&SF	[6.9540, 3.0661]	1	0.9224	0.9831	6.1122	459
MCS	[6.7634, 3.3883]	1	0.9850	0.9850	6.6249	3×10^6

problem, denoted as SPCE&SF. Furthermore, direct Monte Carlo simulation is utilized to verify the accuracy of the proposed method. As shown in Table 2 where the reliability R_1 , R_2 , and R_3 are verified through direct MCS, the SPCE&SF approach obtains an optimum design after 17 iterations while requiring 459 function evaluations in total. However, the resulting optimum design violates the probabilistic constraints as the reliability R_2 and R_3 are less than the target 0.985 and the error of time-variant reliability for performance function G_2 is 6.36%. With the proposed SKM approach, the optimum design is close to the optimum solution obtained from direct MCS and satisfies the reliability requirements. In addition, it is observed that the proposed SKM approach only needs 147 function evaluations to obtain an accurate optimum design, including 27, 84, and 36 function calls for Kriging model g_{K1} , g_{K2} , and g_{K3} , respectively. The results demonstrate that the proposed approach can efficiently handle stochastic processes and solve time-variant RBDO problems effectively.

3.2 Case study II: a cantilever beam design problem

In the second study, a cantilever beam under an external load is introduced as shown in Fig. 12. The material of the beam is assumed to be SAE-1008, a standard grade carbon steel which is widely used in auto manufacture, oil drum, and

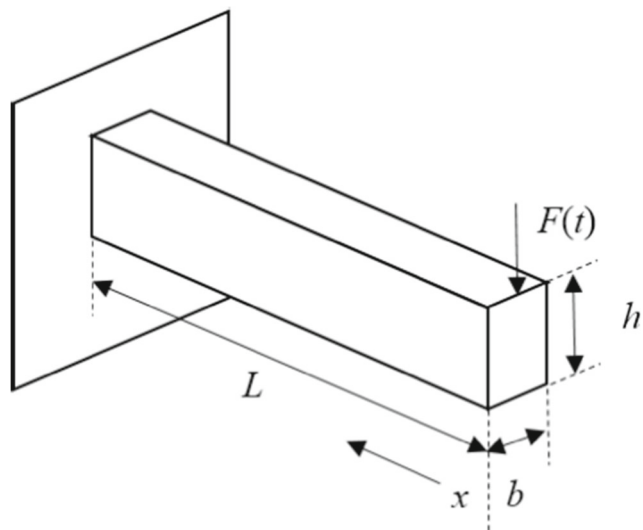


Fig. 12 Geometry of cantilever beam

Table 3 Cantilever beam specifications

Random variable	Distribution	Mean value	Standard deviation
Length, L	/	500 mm	/
Width, b	Normal	b	3.436 mm
Height, h	Normal	h	3.436 mm
External Load $F(t)$	Normal	170 kN	10 kN

transformer’s tank panel. The length L is fixed to 500 mm while height h and width b are treated as two design variables, denoted as $\mathbf{d} = [h, b]$. An external load $F(t)$ is applied on the tip of this beam and depicted as a stationary Gaussian stochastic process with 170 kN mean and 10 kN standard deviation. The time interval of interest is $[0, 1]$, and all random variables and stochastic process are detailed in Table 3.

For this cantilever beam, the stress at position x can be expressed as

$$S(x) = \frac{6 \cdot F(t) \cdot (L-x)}{bh^2} \tag{43}$$

According to the geometry of the beam, the maximum stress at $x = 0$ can be expressed as

$$S_{\max} = S(0) = \frac{6F(t)L}{bh^2} \tag{44}$$

Given the yield strength of SAE-1008 $S_y = 275$ MPa, the limit state function of this beam is defined as

$$G(\mathbf{d}, F(t)) = S_y - S_{\max} \tag{45}$$

Thus, for any time instant t within $[0, 1]$, $G(\mathbf{d}, F(t)) < 0$ indicates failure due to plastic deformation. The size of cross

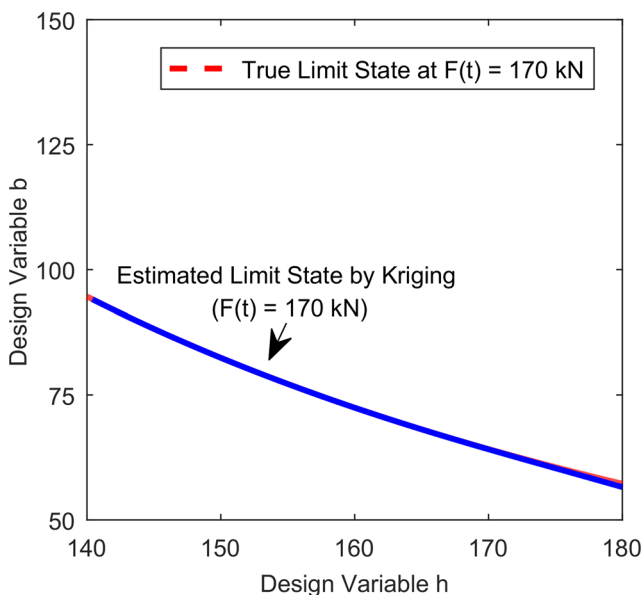


Fig. 13 High fidelity of the updated Kriging model at h, b design space

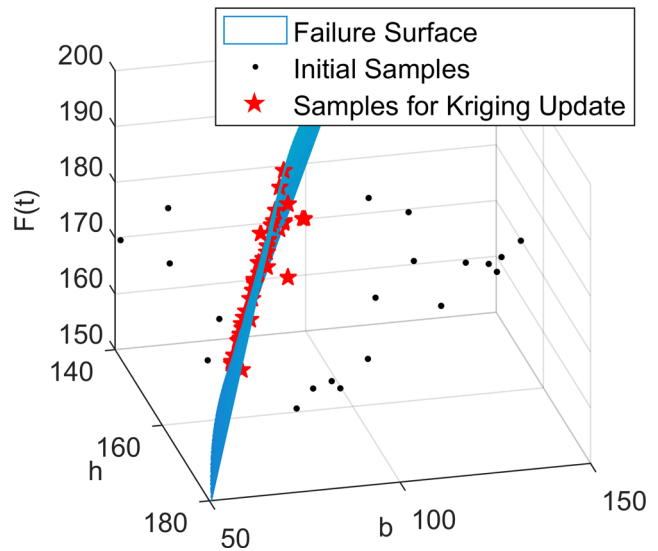


Fig. 14 Sample points for constructing Kriging model

section is formulated as an objective function, and the boundaries of the two design variables are given as 1) the height h should be within $[140, 180]$ in millimeters and 2) the width b should be within $[50, 150]$ in millimeters. Therefore, the cantilever beam tRBDO problem is formulated as

$$\begin{aligned} &\text{Minimize : } \text{Cost}(\mathbf{d}) = h + b \\ &\text{subject to : } P_f(0, 1) = \Pr(\exists t \in [0, 1], G(\mathbf{d}, F(t)) \leq 0) \leq 1 - R_t \\ &\quad \mathbf{d} = [h, b] \\ &\text{where } G = S_y - \frac{6000 \cdot F(t) \cdot 500}{h^2 \cdot b} \end{aligned} \tag{46}$$

In this study, a target reliability is set to $R_t = 0.985$ and a target cumulative confidence level CCL_t is set to 0.999. The deterministic design starts with the mean value of the design variables $\mathbf{d}_0 = [160, 100]$ and terminates at the

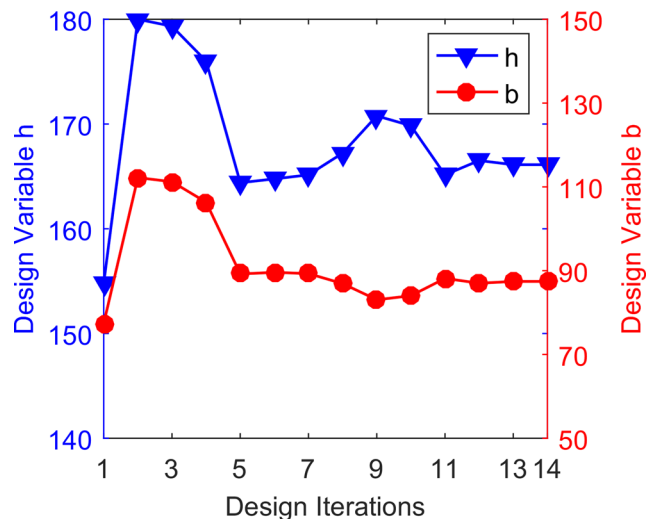


Fig. 15 Design history at each iteration

Table 4 tRBDO design history for case study II

Iterations	Design variables		R^{SKM}	Cost
	h	b		
1	154.7946	77.3973	0.0363	232.1919
2	180.0000	112.2090	1.0000	292.2090
3	179.3359	111.2309	1.0000	290.5669
4	176.0155	106.3408	1.0000	282.3563
5	164.3941	89.2254	0.9789	253.6194
6	164.7613	89.5981	0.9841	254.3594
7	165.1484	89.3034	0.9848	254.4517
8	167.2207	86.9177	0.9852	254.1384
9	170.7791	83.0660	0.9840	253.8451
10	169.8417	84.0105	0.9849	253.8523
11	165.1435	88.1642	0.9830	253.3078
12	166.5170	87.0030	0.9847	253.5200
13	166.1181	87.4380	0.9850	253.5561
14	166.1193	87.4383	0.9850	253.5576

deterministic optimum design $\mathbf{d}_d = [154.7946, 77.3973]$, while 11 points are evaluated during the deterministic optimization process. By employing the stochastic equivalent transformation, the stochastic process $F(t)$ is transformed to a random variable F' , which follows a normal distribution with 170 kN mean and 10 kN standard deviation since $F(t)$ is a stationary Gaussian process. By discretizing the time interval into 100 time nodes, 10^6 random realizations are obtained as introduced in Section 2.2. To solve the tRBDO problem, a total number of 20 initial samples points are generated by Latin hypercube sampling scheme and evaluated for the performance function. The initial Kriging model is then constructed based on the available 31 samples, and 10^6 random realizations of the stochastic process $F(t)$ are generated for the time-variant reliability analysis. The tRBDO process starts with the deterministic optimum design \mathbf{d}_d , and it converges to an optimum design $\mathbf{d}_{opt} = [166.1193, 87.4383]$ after 14 iterations. As shown in Fig. 13, the approximated limit state function is compared with the true responses while the stochastic load is fixed to 170 kN. It shows that the high-fidelity Kriging model is able to accurately approximate limit state functions.

Table 5 Comparison of optimum results for case study II

	Optimum	Reliability	Cost	#F
SKM	[166.1193, 87.4383]	0.9856	253.5576	66
SPCE&SF	[167.7387, 85.6917]	0.9848	253.4304	400
MCS	[168.4629, 84.9994]	0.9850	253.4623	10^6

In the SKM approach, the Kriging model is automatically updated through the design-driven adaptive sampling at each design iteration and a total number of 35 most useful sample points are identified during the overall tRBDO process. All the selected samples for constructing the Kriging model are plotted in Fig. 14, where black nodes represent the initial points and red stars denote the most useful samples. As shown in the figure, almost all the selected samples are located on the failure surface, ensuring an efficient Kriging updating procedure. Figure 15 shows the iterative history of design variables during tRBDO process while Table 4 provides the reliabilities R^{SKM} , design points, and cost at each design iteration.

For the comparison purpose, the SPCE&SF method and direct MCS method are also employed to solve the tRBDO problem for the cantilever beam case study, and the optimum solutions and number of function evaluations from three methods are listed in Table 5. To verify the optimum designs obtained by the SKM and SPCE&SF, MCS with 10^6 samples is employed as the reference to compute the reliabilities. An optimum design is obtained after 40 iterations by SPCE&SF as [167.7387, 85.6917], while 400 function evaluations are required to construct a SPCE model in design optimization. The result shows that both SKM and SPCE&SF approach can accurately solve the time-variant reliability-based design optimization problem involving stationary Gaussian process. However, the SKM approach is more efficient as it only requires 66 functions evaluations for achieving the optimum design.

3.3 Case study III: aircraft tubing design

In industry, tubing assemblies have been widely integrated in many subsystems, for example, fuel system and hydraulic system. Catastrophic system failure can be caused by the potential failure of aircraft tubing, and determining the optimized geometry of tubing under the time-variant uncertainties becomes extremely important in the early design stage. In this study, a twisted tubing design problem is solved by employing the proposed SKM approach.

A twisted tube made of steel ($E = 200$ GPa, $\nu = 0.27$) is shown in Fig. 16. The inner diameter D , thickness T , the radius

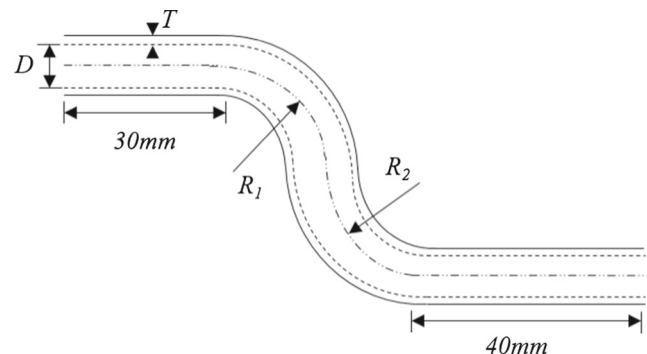
**Fig. 16** Geometry of twisted aircraft tubing

Table 6 Aircraft tubing specifications

Design variable	Distribution	Mean value	STD	Boundary
Inner diameter, D	Normal	μ_D	0.1 mm	[14 mm, 16 mm]
Thickness, T	Normal	μ_T	0.05 mm	[2 mm, 2.6 mm]
Radius of bending, R_1	Normal	μ_{R1}	0.1 mm	[14 mm, 16 mm]
Radius of bending, R_2	Normal	μ_{R2}	0.1 mm	[14 mm, 16 mm]

of bending for two bended tube R_1 and R_2 are design variables that follow normal distributions, detailed in Table 6.

The tube will experience time-variant pressure $P(t)$ during the operation, which is applied on the inner surface of the twisted tube. The inner pressure is modeled as a stationary Gaussian process with 30 MPa the mean and 1 MPa standard deviations respectively. The time interval of interest is $[0, 1]$ and the autocorrelation function of $P(t)$ is the same as shown in (41). A finite element model has been developed in ANSYS to obtain the maximum von Mises stress of the tube. A failure is defined as the maximum von Mises stress is greater than the yield strength $\sigma_y = 235$ MPa, and the design objective is to minimize the total volume of the twisted tube, expressed as

$$\text{Cost}(D, T, R_1, R_2) = \pi \left\{ \left(\frac{D}{2} + T \right)^2 - \left(\frac{D}{2} \right)^2 \right\} \left(30 + 40 + \frac{2\pi R_1}{4} + \frac{2\pi R_2}{4} \right) \tag{47}$$

Thus, the tRBDO problem for the aircraft tubing design is formulated as,

$$\begin{aligned} &\text{Minimize : } \text{Cost}(\mathbf{d}) \\ &\text{subject to : } P_f(0, 1) = \Pr(\exists t \in [0, 1], G(\mathbf{d}, P(t)) \leq 0) \leq 1 - R_t, \\ &\quad \mathbf{d} = [D, T, R_1, R_2] \\ &\text{where } G(\mathbf{d}, P(t)) = \sigma_y - \text{Max}_{\text{stress}}(\mathbf{d}, P(t)) \end{aligned} \tag{48}$$

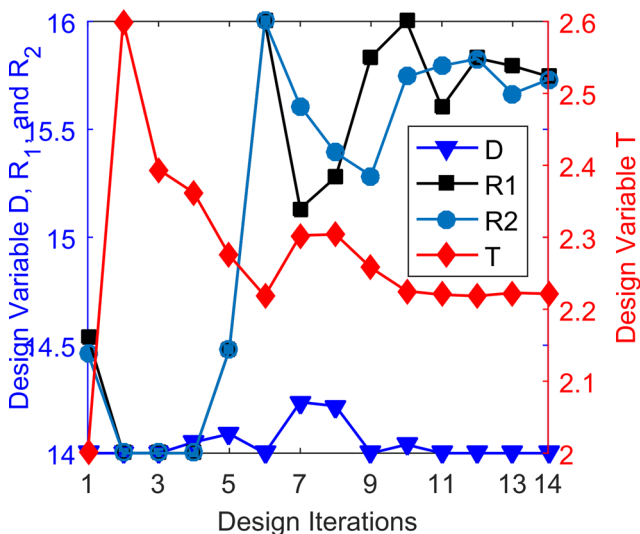


Fig. 17 Design variables in tRBDO

In this study, both the targets of reliability and the cumulative confidence level are set to 0.98. Starting with the design [15, 2.3, 15, 15], a deterministic design optimization problem is first solved to obtain the initial design point for tRBDO. By using the finite difference method to provide the sensitivity, the deterministic solution $\mathbf{d}_d = [14, 2, 14.5420, 14.4637]$ is obtained after 10 iterations, and 50 samples points are evaluated during the deterministic design process. In the SKM approach, the time-variant limit state function with stochastic processes is first converted into time-independent counterpart through the stochastic equivalent transformation. To construct surrogate model for the finite element simulation, an Kriging model is trained based on the 50 sample points that evaluated in deterministic optimization and 40 random samples generated by Latin hyper cube sampling. The time interval $[0, 1]$ is evenly discretized into 100 time nodes, then 10^6 random realizations of the stochastic process $P(t)$ is generated for time-variant reliability analysis. The optimum design is achieved after 14 iterations as $\mathbf{d}_{\text{opt}} = [14.0000, 2.2215, 15.7457, 15.7297]$, and the iterative design history for the four design variables is shown in Fig. 17. The convergence of the time-variant reliability and the total volume of the twisted tube are plotted in Fig. 18.

The design-driven adaptive sampling scheme is employed in the tRBDO to ensure that the CCL of the Kriging model satisfies the target value, and 145 most useful

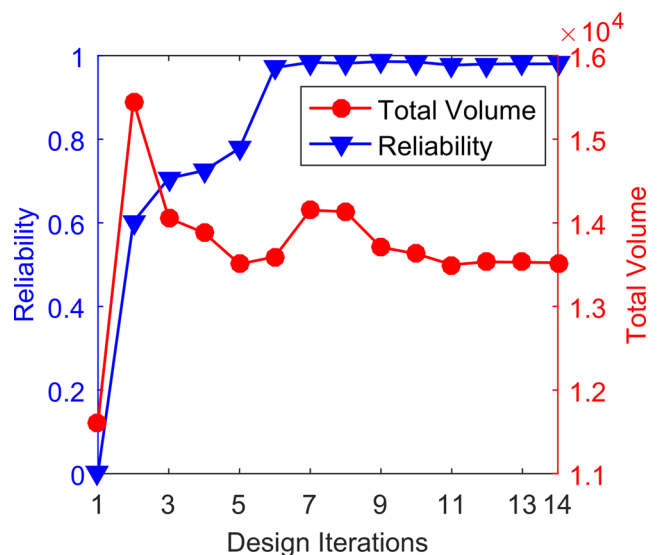


Fig. 18 Reliability and total volume in tRBDO

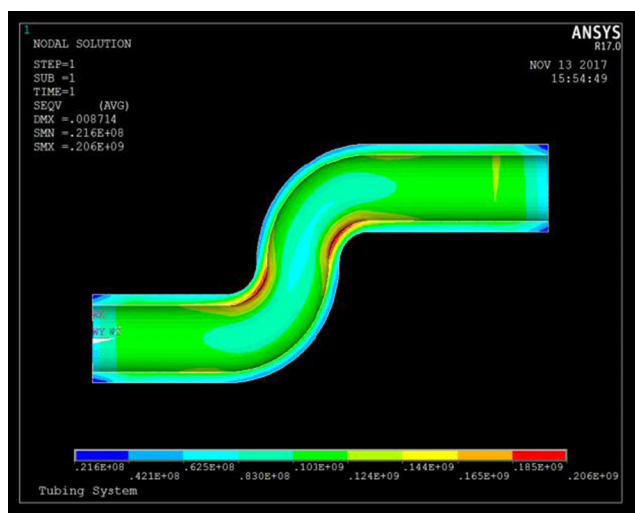


Fig. 19 Stress contour in ANSYS

samples are identified until the optimum design is obtained. With a total number of 235 function evaluations in the tRBDO, the total volume of the twisted tube is minimized to 13,522.173 mm³ while the reliability is approximated as 0.9803. Figure 19 shows the stress contour of the optimum design in ANSYS while the inner stress is set to 30 MPa.

4 Conclusion

This paper presents a sequential Kriging modeling approach to accurately evaluate time-variant reliability and efficiently carry out the time-variant RBDO involving stochastic processes. To reduce the high dimensionality associated with time-variant uncertainties, the SKM approach first converts time-variant limit state functions to time-independent counterparts using stochastic equivalent transformation, and then build Kriging surrogate models to predict the responses of time-variant limit state functions. To enhance the accuracy of time-variant reliability approximations in tRBDO, a design-driven adaptive sampling scheme is developed to update surrogate models by identifying most useful sample points within time-variant random space. As a result, the system failures can be captured with the high-fidelity Kriging models to predict the time-variant reliability in MCS. With the sensitivity information obtained by the first-order score function, sequential quadratic programming (SQP) is adopted as an optimizer to search for optimal solutions iteratively. The results of three case studies indicate that the sequential Kriging modeling approach is capable of effectively handling tRBDO problems involving stochastic processes.

References

- Agarwal H, Renaud JE (2006) New decoupled framework for reliability-based design optimization. *AIAA J* 44(7):1524–1531
- Andrieu-Renaud C, Sudret B, Lemaire M (2004) The PHI2 method: a way to compute time-variant reliability. *Reliab Eng Syst Saf* 84(1):75–86
- Baran I, Tutum CC, Hattel JH (2013) Reliability estimation of the pultrusion process using the first-order reliability method (FORM). *Appl Compos Mater* 20(4):639–653
- Chen J-B, Li J (2007) The extreme value distribution and dynamic reliability analysis of nonlinear structures with uncertain parameters. *Struct Saf* 29(2):77–93
- Du X, Hu Z (2012) First order reliability method with truncated random variables. *J Mech Des* 134(9):091005
- Gaspar B, Teixeira A, Soares CG (2014) Assessment of the efficiency of Kriging surrogate models for structural reliability analysis. *Probab Eng Mech* 37:24–34
- Ghanem RG, Spanos PD (2003) *Stochastic finite elements: a spectral approach*. Courier Corporation, North Chelmsford
- Hu Z, Du X (2012) Time-dependent reliability analysis by a sampling approach to extreme values of stochastic processes. ASME Paper No. DETC2012-70132
- Hu Z, Du X (2015) First order reliability method for time-variant problems using series expansions. *Struct Multidiscip Optim* 51(1):1–21
- Hu C, Youn BD (2011) Adaptive-sparse polynomial chaos expansion for reliability analysis and design of complex engineering systems. *Struct Multidiscip Optim* 43(3):419–442
- Hu Z, Li H, Du X, Chandrashekhara K (2013) Simulation-based time-dependent reliability analysis for composite hydrokinetic turbine blades. *Struct Multidiscip Optim* 47(5):765–781
- Hu Z, Mahadevan S, Du X (2016) Uncertainty quantification of time-dependent reliability analysis in the presence of parametric uncertainty. *ASCE-ASME J Risk Uncertainty Eng Syst Part B Mech Eng* 2(3):031005
- Kim NH, Wang H, Queipo NV (2006) Adaptive reduction of random variables using global sensitivity in reliability-based optimisation. *Int J Reliab Saf* 1(1–2):102–119
- Kuschel N, Rackwitz R (2000a) Optimal design under time-variant reliability constraints. *Struct Saf* 22(2):113–127
- Kuschel N, Rackwitz R (2000b) Time-variant reliability-based structural optimization using SORM. *Optimization* 47(3–4):349–368
- Li C-C, Der Kiureghian A (1995) Mean out-crossing rate of nonlinear response to stochastic input. *Proceedings of ICASP-7, Balkema, Rotterdam*, pp 295–302
- Li M, Wang Z (2017) Sequential kriging optimization for time-variant reliability-based design involving stochastic processes. *Proc. ASME 2017 International Design Engineering Technical Conferences and Computers and Information in Engineering Conference*, American Society of Mechanical Engineers, pp. V02AT03A042-V002AT003A042
- Li J, Chen J-B, Fan W-L (2007) The equivalent extreme-value event and evaluation of the structural system reliability. *Struct Saf* 29(2):112–131
- Li F, Wu T, Badiru A, Hu M, Soni S (2013) A single-loop deterministic method for reliability-based design optimization. *Eng Optim* 45(4):435–458
- Lin PT, Gea HC, Jaluria Y (2011) A modified reliability index approach for reliability-based design optimization. *J Mech Des* 133(4):044501
- Majcher M, Mourelatos ZP, Geroulas V, Baseski I, Singh A (2015) An efficient method to calculate the failure rate of dynamic systems with random parameters using the total probability theorem. *Army Tank Automotive Research Development and Engineering Center, Warren*

- Mansour R, Olsson M (2016) Response surface single loop reliability-based design optimization with higher-order reliability assessment. *Struct Multidiscip Optim* 54(1):63–79
- Nocedal J, Wright SJ (2006) *Sequential quadratic programming*. Springer, Berlin
- Rahman S, Xu H (2004) A univariate dimension-reduction method for multi-dimensional integration in stochastic mechanics. *Probab Eng Mech* 19(4):393–408
- Sakamoto S, Ghanem R (2002a) Simulation of multi-dimensional non-Gaussian non-stationary random fields. *Probab Eng Mech* 17(2): 167–176
- Sakamoto S, Ghanem R (2002b) Polynomial chaos decomposition for the simulation of non-Gaussian nonstationary stochastic processes. *J Eng Mech* 128(2):190–201
- Saul LK, Jordan MI (1999) Mixed memory markov models: decomposing complex stochastic processes as mixtures of simpler ones. *Mach Learn* 37(1):75–87
- Shan S, Wang GG (2008) Reliable design space and complete single-loop reliability-based design optimization. *Reliab Eng Syst Saf* 93(8): 1218–1230
- Simpson TW, Martins JR (2011) Multidisciplinary design optimization for complex engineered systems: report from a national science foundation workshop. *J Mech Des* 133(10):101002
- Singh A, Mourelatos ZP, Li J (2010) Design for lifecycle cost using time-dependent reliability. *J Mech Des* 132(9):091008
- Singh A, Mourelatos ZP, Nikolaidis E (2011) An importance sampling approach for time-dependent reliability. *Proc. Proceedings of the ASME 2011 International Design Engineering Technical Conferences and Computers and Information in Engineering Conference, IDETC/CIE*, pp 28–31
- Stein M (1988) Asymptotically efficient spatial interpolation with a misspecified covariance function. *Ann Stat* 16:55–63
- Sudret B (2008) Analytical derivation of the outcrossing rate in time-variant reliability problems. *Struct Infrastruct Eng* 4(5):353–362
- Wang Z, Chen W (2016) Time-variant reliability assessment through equivalent stochastic process transformation. *Reliab Eng Syst Saf* 152:166–175
- Wang Z, Chen W (2017) Confidence-based adaptive extreme response surface for time-variant reliability analysis under random excitation. *Struct Saf* 64:76–86
- Wang Z, Wang P (2013) A new approach for reliability analysis with time-variant performance characteristics. *Reliab Eng Syst Saf* 115: 70–81
- Wang Z, Wang P (2015) A double-loop adaptive sampling approach for sensitivity-free dynamic reliability analysis. *Reliab Eng Syst Saf* 142:346–356
- Wang Y, Zeng S, Guo J (2013) Time-dependent reliability-based design optimization utilizing nonintrusive polynomial chaos. *J Appl Math* 2013:561–575
- Won J, Choi C, Choi J (2009) Improved dimension reduction method (DRM) in uncertainty analysis using kriging interpolation. *J Mech Sci Technol* 23(5):1249–1260
- Wu Y-T, Shin Y, Sues RH, Cesare MA (2001) Safety-factor based approach for probability-based design optimization. *Proc. AIAA/ASME/ASCE/AHS/ASC Structures, Structural Dynamics, and Materials Conference and Exhibit, 42nd, Seattle*
- Yang D, Yi P (2009) Chaos control of performance measure approach for evaluation of probabilistic constraints. *Struct Multidiscip Optim* 38(1):83
- Youn BD, Choi KK, Du L (2005) Enriched performance measure approach for reliability-based design optimization. *AIAA J* 43(4): 874–884
- Yu X, Du X (2006) Reliability-based multidisciplinary optimization for aircraft wing design. *Struct Infrastruct Eng* 2(3–4):277–289
- Zhang J, Du X (2011) Time-dependent reliability analysis for function generator mechanisms. *J Mech Des* 133(3):031005
- Zhang J, Ellingwood B (1994) Orthogonal series expansions of random fields in reliability analysis. *J Eng Mech* 120(12):2660–2677
- Zhang D, Han X, Jiang C, Liu J, Li Q (2017) Time-dependent reliability analysis through response surface method. *J Mech Des* 139(4): 041404
- Zou T, Mahadevan S (2006) A direct decoupling approach for efficient reliability-based design optimization. *Struct Multidiscip Optim* 31(3):190–200